Superconducting Magnet Radiation Effects in Fusion Reactors

Mohamed E. Sawan
Peter L. Walstrom

June 1986

UWFDM-703

Presented at the 7th Topical Meeting on the Technology of Fusion Energy, Reno, Nevada, 15–19 June 1986; Fus. Tech. 10/3 (1986) 741.

FUSION TECHNOLOGY INSTITUTE

UNIVERSITY OF WISCONSIN

MADISON WISCONSIN

Superconducting Magnet Radiation Effects in Fusion Reactors

Mohamed E. Sawan, Peter L. Walstrom

Fusion Technology Institute
University of Wisconsin
1500 Engineering Drive
Madison, WI 53706

June 1986

UWFDM-703

Presented at the 7th Topical Meeting on the Technology of Fusion Energy, Reno, Nevada, 15–19 June 1986; Fus. Tech. 10/3 (1986) 741.

SUPERCONDUCTING MAGNET RADIATION EFFECTS IN FUSION REACTORS

MOHAMED E. SAWAN and PETER L. WALSTROM, University of Wisconsin
Fusion Technology Institute, Nuclear Engineering Department
1500 Johnson Drive, Madison, WI 53706-1687
(608) 263-5093 or (608) 263-3143

ABSTRACT

Radiation effects in superconducting magnets of fusion reactors are analyzed and experimental data reviewed. The interaction between the different radiation effects and impact on reactor design is discussed. The need for experimental data with higher irradiation levels is assessed.

I. INTRODUCTION

The radiation limits for the magnets determine the shield thickness that directly influences the cost of electricity. The superconducting magnet components most sensitive to radiation damage are the superconductor filaments, stabilizer, and electrical and thermal insulators. In addition to its effect on winding temperatures, nuclear heating affects the economic performance of the reactor through increased refrigeration costs. In the past most researchers considered these effects separately. Recently, the relative radiation sensitivity of the various magnet components was assessed.[1] This depends on the radiation limits and the magnet design.

Radiation effects are related as they are determined by the flux level in the magnet. Reviewing previous magnet shielding neutronics calculations for the different conceptual fusion reactor designs,[2] we found a rule-of-thumb relation for radiation effects that holds to within a factor of two. For a 30 full power year (FPY) exposure to the nuclear radiation leaking from the back of the shield, a peak winding pack power density of 1 mW/cm^3 corresponds to $\sim 10^{-3}$ dpa/FPY in the copper stabilizer, $\sim 5 \times 10^{23}$ n/m^2 (E > 0.1 MeV) end of life fluence and $\sim 5 \times 10^{10}$ rad end of life insulator dose. Hence, in efforts to push radiation limits, the different magnet radiation effects should be considered simultaneously. In this paper, we review the most recent irradiation data and assess the need for performing experiments with higher irradiation levels. The interaction between radiation effects as well as the influence of magnet design will be discussed.

II. RADIATION EFFECTS ON SUPERCONDUCTORS

These effects are related to the damage produced by fast neutrons through the production of defect cascades.[3] The damage is usually measured in damage energy available per atom in eV/atom. The total damage energy is the integral over all neutron energies of the product of the damage energy cross section and neutron flux. Due to the steep variation with energy of the damage energy cross section, different damage will be produced if the superconductor is exposed to the same neutron fluence in different facilities with different neutron spectra.

Degradation of critical properties is usually related to fast neutron fluence (E > 0.1 MeV). To compare irradiation experiments in different facilities, knowledge of the neutron spectrum is required. The relative number of neutrons that produces equal damage in superconductors as that produced by one neutron in RTNS-II was calculated by Guinan and co-workers[3,4,5] to be 4.5, 5.74, 7, 3.68, and 4.7 for IPNS, HFBR, TFCX, STARFIRE and MARS, respectively. We calculated the relative number for the MINIMARS[2] central cell magnets to be 5.1.

Available experimental results on NbTi alloys indicate that while the critical temperature (T_c) and upper critical magnetic field (H_{c2}) are insensitive to damage, the critical current density (J_c) degrades with neutron fluence. The J_c degradation from irradiation at HFBR reactor ambient temperature[6] is plotted in Fig. 1 versus damage energy; J_c saturates at 80% of its pre-irradiation value at high fluence. The effect of irradiation temperature is small, as can be seen on the left hand side of Fig. 1.[7] The lowest curve (Swiss LCT conductor) lacks high-fluence data but appears to be leveling off at high fluence. If J_c does saturate after 4 K irradiation, fluences as high as 10^{26} n/m^2 will not have significant effect on critical

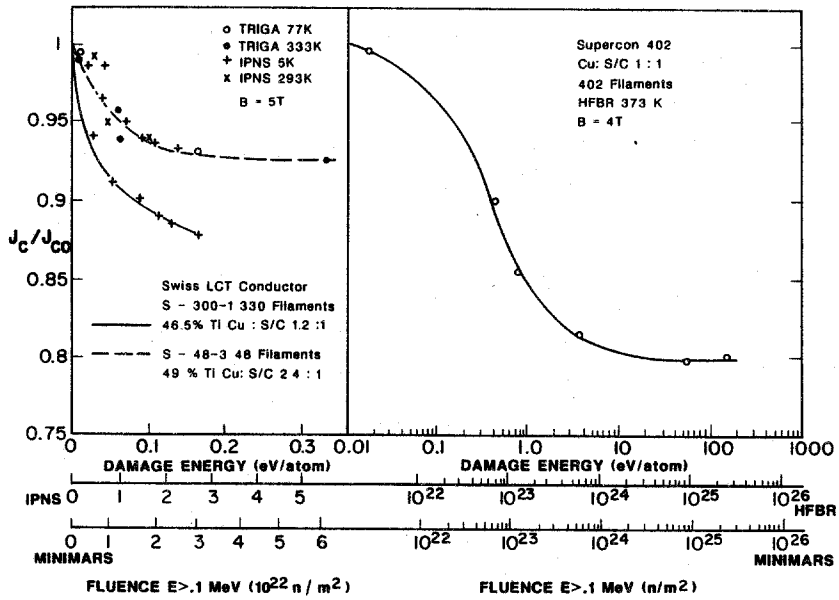

Fig. 1. Degradation of J_c in NbTi as function of damage energy and equivalent neutron fluence.

properties of NbTi and no practical limit is needed. Notice that a conservative fluence limit of 3 x 10^{22} n/m^2 (the highest fluence used in 4 K irradiations) coupled with 70% recovery with room temperature annealing, implies end-of-life fluence limit of ~ 10^{23} n/m^2.

Radiation effects for A15 compounds are different because of the long-range ordered atomic structure. Most experimental data involve irradiation at fission reactor ambient temperatures[5] with few low fluence 4 K irradiation data.[4] T_c is nearly constant up to a fluence of ~ 10^{22} n/m^2 and drops rapidly at higher fluences.[4] All T_c data from irradiating in different facilities at different temperatures agree when compared on a damage energy basis.[4] Recent data for 19-core and commercial 10,000-filament Nb_3Sn wires[8] agree also very well with previous monofilament data. The drop in T_c is less than 3% up to a fusion reactor fluence (E > 0.1 MeV) of ~ 5 x 10^{22} n/m^2 and increases to ~ 20% at ~ 2 x 10^{23} n/m^2. In general, an initial rise in J_c was observed with a subsequent drop at higher fluences. The initial rise, which is related to increased H_{c2} with nearly constant T_c at low fluences, increases for larger fields and lower irradiation temperatures.[7,9] H_{c2} was found to vary with fluence in a similar fashion.[8]

Figure 2 shows the experimental data for the effect of irradiation on J_c compared on a damage energy basis. Comparing the results of high temperature HFBR irradiation[5] with the 4 K irradiation of the nearly identical monofilament sample[4] indicates that high temperature irradiation yields larger J_c degradation. This is due to defect mobility and subsequent cascade collapse during the high temperature irradiation resulting in lower flux pinning. Hence, using the high temperature irradiation data yields conservatively low fluence limits. The commercial 10,000-filament wires[8] have less J_c degradation than the 19-core wires.[5,9] Based on the high temperature irradiation data for multifilamentary wires, a conservative fluence limit of 10^{23} n/m^2 can be used. However, this needs to be confirmed by 4 K irradiation data. It was observed that J_c variation with fluence depends on the method of preparing the superconductor, implying that higher fluence limits might be possible if Nb_3Sn is properly optimized for nuclear applications. Preliminary 4 K irradiation data for ternary alloyed Nb_3Sn wires indicate that these materials have a peak J_c at ~ 1/2 the fluence at which J_c peaks for Nb_3Sn.[8] Hence, a lower fluence limit should be used for these wires.

III. RADIATION EFFECTS ON ORGANIC INSULATORS

The mechanical and dielectric strength and resistivity of the insulators are the important properties. Experimental data for fiber-reinforced organic insulators indicate that the mechanical properties degrade at a lower dose than do the electrical ones.[1] Polyimides are 5 to 10 times more radiation resistant than epoxies.[10] Samples of several millimeters-thick cylindrical rods of glass-fiber-filled (gff) polyimide were irradiated by gamma rays at 5 K and tested for flexural and compression strength.[10] More than 65% of the strength was

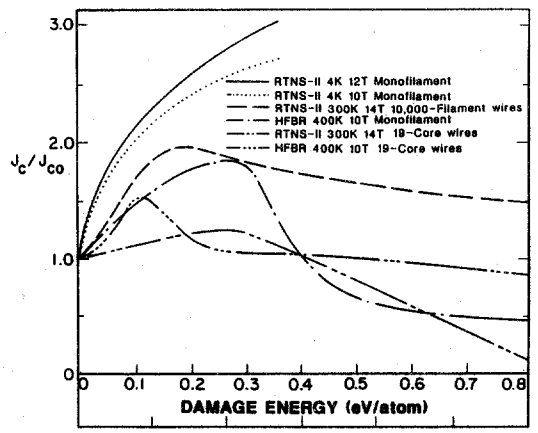

RTNS	0	0.5	1.0	1.5	2	2.5	3
MINIMARS	0	2.55	5.1	7.65	10.2	12.75	15.3
HFBR	0	2.85	5.7	8.55	11.4	14.25	17.1

Fig. 2. J_c changes in Nb_3Sn as function of damage energy and equivalent neutron fluence.

retained up to a dose of ~ 10^{10} rad. The samples are representative of relatively thick sheets of insulators placed between conductors with both compression and interlaminar shear being important.

Recently, 0.5 mm-thick disks of gff polyimide (Spaulrad-S) were irradiated at 325 K to a mixed gamma and neutron dose of ~ 4 x 10^{11} rad with no failures observed in the static compression tests with 275 MPa stress level.[11] In these tests essentially no interlaminar shear occurred. These results are applicable to designs with compressive strains only. In addition, no voltage breakdown data were taken. In general, experimental data for cryogenic irradiation of insulators with the proper mix of gamma and neutron doses (90% neutrons) are needed. A dose limit of 4 x 10^{11} rad can be used if the magnet is designed with the insulator loaded in compression only. Potential insulator material improvements can lead also to higher dose limits. It should be emphasized that this dose level corresponds to an excessive neutron fluence of 4 x 10^{24} n/m^2, implying that one might not need to push the insulator dose that far.

Aluminized mylar has been used in previous designs as thermal insulator. However, recent experiments showed a large drop in its strength after irradiation to 6 x 10^8 rads.[12] No failure of any type was observed in aluminized Kapton up to a dose of 10^{10} rads.[12] The superinsulator located in front of the magnet case is exposed to doses higher than those in the electrical insulators. The more radiation resistant aluminum sheets supported with glass paper can be used with essentially no practical dose limit.

IV. RADIATION EFFECTS ON STABILIZERS

Neutron irradiation at cryogenic temperature produces immobile point defects in the stabilizer resulting in a zero-field radiation induced resistivity $\Delta\rho_r$ which impacts the total resistivity at field. The relation between $\Delta\rho_r$ and Cu dpa is[13]

$$\Delta\rho_r = 3 \times 10^{-9} \left[1 - e^{-240 \times \text{dpa}}\right] \Omega\text{m} . \quad (1)$$

The stabilizer resistivity increase can be accommodated by making the current density lower and the outer radius larger. The cost impact is mainly in the increased mass of the magnets themselves. In tokamaks, increasing the winding cross-section impacts most machine parameters with a much larger cost impact.

The resistivity at the operating field ρ_D depends on $\Delta\rho_r$ and the purity of Cu. Furthermore, partial recovery (80-90%) of radiation induced defects can be achieved by room temperature annealing. Based on Kohler's plot for Cu, we generated a chart relating $\Delta\rho_r$ to ρ_D given the field B[14] and the residual resistivity ratio RRR of Cu.[14] The dpa rate limit is determined by dividing the dpa limit, from Eq. (1), by the time before the first magnet anneal. Power reactor availability considerations require at least 5 FPY's before the first magnet anneal.

In assessing the effect of stabilizer resistivity increases, the magnet designer must consider both magnet stability and protection. For cryostatically stable He-I designs, the best performance to date is about 3 x 10^7 A/m^2 at 8 T;[15] by scaling from this datum one can write

$$j^{max} = 3 \times 10^7 \left[\frac{4.8 \times 10^{-10}}{\rho_D}\right]^{1/2} \text{A/m}^2 \quad (2)$$

where ρ_D is in Ωm. For fluences of the level of the MINIMARS design, ρ_D is 10^{-9} Ωm and j^{max} for a cryostatically stable design is 1.8 x 10^7 A/m^2. The protection limit, on the other hand, is a function of the coil inductance and allowable dump voltage, as well as the stabilizer resistivity. The protection limit is determined by the final temperature reached by a normal zone present at the beginning of an emergency coil discharge; this temperature is affected by heating rate, specific heats, and dump time.

For fixed winding pack dimensions and current density (fixed field), the inductance L scales as I^2. The dump time constant τ is given by the expression

$$\tau = L_o I_o^2 / I\, V_D \quad (3)$$

where I_o and L_o are datum values, V_D the dump voltage and I the variable operating current. This shows that for protection purposes it is desirable to increase I and V_D. The current is limited by manufacturing, stability and lead loss considerations; V_D is limited by dielectric breakdown strength to a few thousand volts for bath-cooled coils and tens of thousands of volts for force-cooled coils. The allowable average current density is given by the formula

$$j_{av} = [2f_{cu}f_{co}I(T_f)/\tau]^{1/2} \qquad (4)$$

where f_{cu} is the copper fraction, f_{co} the conductor fraction and $I(T_f)$ is given by:

$$I(T_f) = \int_{T_i}^{T_f} \frac{S_{co}(T)}{\rho_{cu}(T,B)}\, dT \ . \qquad (5)$$

S_{co} is the volumetric specific heat of the conductor.

In general, j_{av} set by protection has a weaker ρ_D dependence than $\rho_D^{-1/2}$ scaling of cryostability, since the integral tends to weight higher temperatures where the ideal copper resistivity becomes large compared to $\Delta\rho_r$; that is, the protection-limited current density falls off more slowly with increasing $\Delta\rho_r$ than stability-limited current density. The protection-limited current density can therefore stay above the cryostable current density limit as ρ_D increases, or intersects it, depending upon the starting values of the two curves.

With pressurized He-II (superfluid) cooling, the mechanism of heat removal is very different from that in boiling He-I, with heat removal being dominated by nonlinear Gorter-Mellink heat conduction in the cooling channels. With proper designs, current densities twice as high or more as those achievable in He-I bath-cooled can be achieved for the same stabilizer resistivity. Nevertheless, the resistivity dependence of the stable current density is $\rho_D^{-1/2}$. Coil protection is determined by the same considerations (Eqs. 3-5) as for the He-I bath-cooled case (again neglecting the effect of the helium, assuming it is blown away from a hot spot). This means that if the current density is raised to take advantage of the greater heat-removal capabilities of He-II, the coil is more likely to be closer to or to exceed the protection limit set by Eqs. (3-5).

A third design approach is the force-flow cable-in-conduit. In this conductor type, a twisted cable of superconductor stabilizer composite wires is completely enclosed by an alloy conduit. The helium coolant, usually at supercritical pressure (P > 2.2 atm), flows between the cable strands. Researchers at MIT and ORNL found that at low flow rates, the stability margin is large (hundreds of mJ/cm^3) for low currents and drops sharply at a limiting current to values of tens of mJ/cm^3. At higher flow rates, the drop is not as large, and at sufficiently high flow rates, the stability margin varies smoothly with current.

Miller, Lue and Dresner[16,17] have given an approximate scaling formula for the limiting current:[18]

$$j_{lim} \sim \left[\frac{f_{cu}f_{co}(1-f_{co})(T_c(B) - T_b)}{\rho_D(B)}\right]^{1/2} \times t^{-1/15}\, l^{2/15}\, d^{-1} \qquad (11)$$

where T_b is the coolant temperature, t the pulse time, l the heated length, and d the hydraulic diameter. As before the current density scales as $\rho_D^{-1/2}$. The allowable current density, however, is higher before irradiation than for cryostatically stable magnets and remains higher as ρ_D increases. Also, the stability margin above the limiting current can be increased by increasing the flow rate. Operation above the limiting current can be considered for many applications; in this case, the protection limit determines the operating current.

The protection analysis of force-flow magnets proceeds as before, except that the quench pressure limit is taken together with nuclear heating considerations to determine the flow path length. Since the helium is confined, some of the ohmic heat is absorbed by the helium and conduit wall; Eq. (5) can be modified to take this into account. In the analysis of the central cell magnets of MINIMARS, an approximate solution was obtained by assuming isochoric heating until the maximum quench pressure was reached and constant pressure heating thereafter. The results of the above analysis are shown in Fig. 3. The addition of the helium term tends to weight the early time, low temperature part of the integral, making the ρ_D dependence closer to $\rho_D^{-1/2}$ than in the adiabatic (no helium) case. Finally, it should be noted that since the resistivity does not increase once the saturation value has been reached, if the current density limits corresponding to this value are acceptable, the magnet can be operated with practically no restriction on stabilizer irradiation.

V. NUCLEAR HEATING

In all of the three cooling schemes previously discussed, bulk heat removal requirements dictate local surface heat fluxes due to nuclear heating smaller than the ohmic heating fluxes considered in a stability analysis. The major

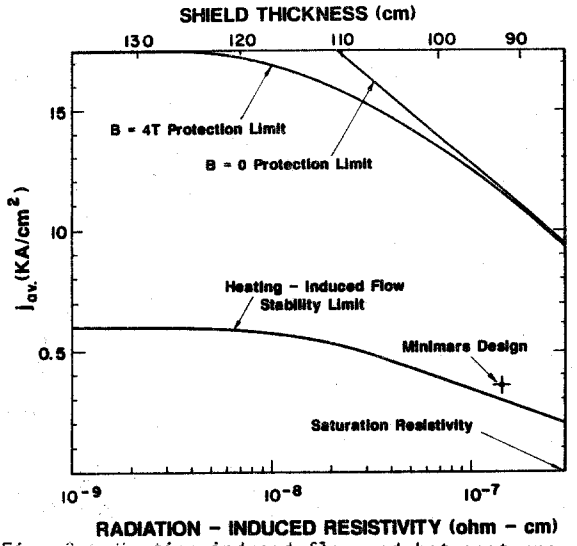

Fig. 3. Heating-induced flow and hot-spot protection current density limits for the central cell magnets of MINIMARS as a function of radiation-induced resistivity and shield thickness.

design impacts are economics and changes in coolant properties and superconductor parameters as a result of temperature changes.

In He-I bath-cooled designs, the impact of bulk heating is mainly that of vapor formation; the designer must ensure that no part of the windings is inadequately supplied with helium liquid. With pressurized He-II cooling, nuclear heating results in a temperature gradient between the regions where such heating occurs and the manifolds where heat is removed; the higher local operating temperature must be taken into account in the design. Similarly, in force-flow magnets, nuclear heating causes an increase in the coolant/conductor temperature as the coolant absorbs heat between the inlet and outlet.

The economic optimum nuclear heating level can be determined by a cost tradeoff analysis, where the total cost of items strongly affected by the shield thickness is minimized. In an axisymmetric configuration such as in tandem mirrors, these are the shield itself, the magnets, and the cryoplant. In toroidal devices, practically all major machine components are affected by shield thickness, and the resultant optimum nuclear heating level is higher. The optimum nuclear heating must then be compared to technical limits.

We performed such an economic tradeoff study on the central cell magnets of MINIMARS using one-dimensional neutronics calculations for nuclear heating and dpa estimates (see Fig. 4). The figure of merit used was incremental cost of the affected components per net electric power. Cryoplant power consumption was

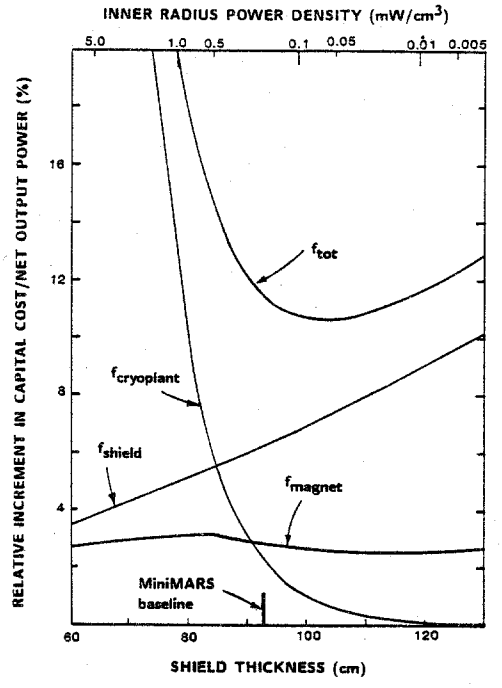

Fig. 4. Fractional changes in capital cost/unit net electric power as a function of shield thickness for MINIMARS components affected by shield thickness.

taken into account by subtracting it from the net output power of the device (600 MW_e). Magnet costs were taken to be \$46/kg; the winding pack current density was taken to be the protection limit as given in Fig. 3. A fixed capital cost of \$1100/W_e at 4 K was used for the cryoplant; its efficiency was taken to be 330 W_e/W. Even if an economic tradeoff analysis indicates that average radiation levels lower than the technical limits should be used, allowance still should be made for hot spots in the magnet. In MINIMARS, such hot spots occur behind coolant manifolds. Hot spot factors as high as five can be expected in fusion reactors.

VI. CONCLUSIONS

Radiation effects in the superconducting magnets of fusion reactors are related. Hence, the radiation limits should be considered simultaneously. Currently available irradiation data indicate that end-of-life fast neutron fluences up to 10^{23} n/m^2 (E > 0.1 MeV) in a fusion reactor will not result in significant degradation in superconductor critical properties. Experimental data on mechanical strength degradation for organic insulators with cryogenic temperature irradiation indicate an end-of-life dose

limit of 10^{10} rads for polyimides. Stabilizer resistivity increase due to radiation damage affects achievable current densities both through reduction in stability margin and in increase in hot-spot temperature during a dump. Force-flow and He-II-cooled designs allow fairly high current densities in spite of large resistivity increases.

The optimum nuclear heating level determined from cost trade-off analysis is design dependent. Accounting for hot spot factors as high as 5 in fusion reactor magnets, we conclude that for the optimum design of axisymmetric fusion reactors hot spot values for fast neutron fluence (E > 0.1 MeV), insulator dose, and Cu radiation induced resistivity of 5×10^{23} n/m^2, 5×10^{10} rad, and 230 nΩcm should be tolerable. The superconducting magnet development program should, therefore, aim at testing magnet components to these levels of irradiation under realistic fusion reactor environmental conditions. Data on the effect of these irradiation levels on the mechanical properties of the magnet structural materials are also essential. Higher radiation levels might be needed in toroidal facilities.

ACKNOWLEDGEMENT

Support provided by U.S. Department of Energy.

REFERENCES

1. R. VAN KONYNENBURG and M. GUINAN, "Relative Radiation Sensitivity of Insulators, Stabilizers, and Superconductors," UCID-19292, Lawrence Livermore National Lab. (1982).

2. J.D. LEE et al., "MINIMARS Final Report," UCID-20773, Lawrence Livermore National Laboratory (1986).

3. P. HAHN, H. WEBER, M. GUINAN et al., "Neutron Irradiation of Superconductors and Damage Energy Scaling of Different Neutron Spectra," UCRL-93186, Lawrence Livermore National Lab. (1985).

4. M. GUINAN, R. VAN KONYNENBURG, J. MITCHELL, et al., "Effects of Low-Temperature Fusion Neutron Irradiation on Critical Properties of a Monofilament Nb_3Sn Superconductor," UCID-20048, Lawrence Livermore National Lab. (1984).

5. C. SNEAD, D. PARKIN, M. GUINAN, "High Energy Neutron Damage in Nb_3Sn: Changes in Critical Properties, and Damage Energy Analysis," J. Nucl. Mat., 103 & 104, 749 (1981).

6. D. PARKIN, A. SWEEDLER, "Neutron Irradiation of Nb_3Sn and NbTi Multifilamentary Composites," IEEE Trans. Magn. MAG-11, 166 (1975).

7. H. WEBER, "Irradiation Damage in Superconductors," Proc. CEC/ICMC Meeting on Advances in Cryogenic Engineering, Cambridge, MA, August 12-16, 1985.

8. R. FLÜKIGER, W. MAURER, W. WEISS, KfK, Karlsruhe, Germany, Private Communications (May 1986).

9. S. SNEAD, JR., D. PARKIN, "Effect of Neutron Irradiation on the Critical Current of Nb_3Sn at High Magnetic Fields," Nucl. Technology, 29, 264 (1976).

10. R. COLTMAN, C. KLABUNDE, "Mechanical Strength of Low-Temperature-Irradiated Polyimides: A Fire-to-Tenfold Improvement in Dose Resistance over Epoxies," J. Nucl. Mat., 103 & 104, 717 (1981).

11. R. SCHMUNK et al., "Tests on Irradiated Magnet Insulator Materials," J. Nucl. Mat., 122 & 123, 1381 (1984).

12. C. LONG et al., "Effects of Radiation at 5 K on Organic Insulators for Superconducting Magnets," Special Purpose Materials Progress Report, U.S. DOE Report DOE-ER0O4811, pp. 73 (1981).

13. M. GUINAN, Lawrence Livermore National Laboratory, Private Communications, June 1983.

14. M. SAWAN, "Charts for Specifying Limits on Copper Stabilizer Damage Rate," J. Nucl. Mat., 122 & 123, 1376 (1984).

15. P.L. WALSTROM, "Stability Limit Guidelines for Superconducting Coil Design," University of Wisconsin Fusion Technology Institute Report UWFDM-611 (Mar. 1985).

16. J.W. LUE, J.R. MILLER, "Heated Length Dependence of the Stability of an Internally Cooled Superconductor," Proc. 9th Symp. on Engineering Problems of Fusion Research, IEEE Publ. No. 81CH1715-2 NPS, New York (1981) p. 652.

17. L. DRESNER, "Superconductor Stability, 1983: A Review," Cryogenics, June 1984, p. 283.

18. J.R. MILLER, J.W. LUE, "Stability of Cable-in-Conduit Superconductors," J. Appl. Phys., 51, No. 1, p. 772.